Planet. Space Sci., Vol. 24, pp. 1007 to 1024. Pergamon Press, 1976. Printed in Northern Ireland

MAGNETOSPHERIC CHORUS: OCCURRENCE PATTERNS AND NORMALIZED FREQUENCY

W. J. BURTIS and R. A. HELLIWELL
Radioscience Laboratory, Stanford University, Stanford, CA 94305, U.S.A.

(*Received in final form* 29 *March* 1976)

Abstract—New characteristics of VLF chorus in the outer magnetosphere are reported. The study is based on more than 400 hours of broadband (0.3–12.5 kHz) data collected by the Stanford University/Stanford Research Institute VLF experiment on OGO 3 during 1966–67. Bandlimited emissions constitute the dominant form of whistler-mode radiation in the region $4 \lesssim L \lesssim 10$. Magnetospheric chorus occurs mainly from 0300 to 1500 LT, at higher L at noon than at dawn, and moves to lower L during geomagnetic disturbance, in accord with ground observations of VLF chorus. Occurrence is moderate near the equator, lower near 15°, and maximum at high latitudes (far down the field lines). The centre frequency f of the chorus band varies as L^{-3} and at low latitudes is closely related to the electron gyrofrequency on the dipole field line through the satellite. Based on the measured local gyrofrequency f_H, the normalized frequency distribution of chorus observed within 10° of the dipole equator shows two peaks, at $f/f_H \cong 0.53$ and $f/f_H \cong 0.34$. This bimodal distribution is a persistent statistical feature of near equatorial chorus, independent of L, LT and K_p. However there is considerable variability in individual events, with chorus often observed above, below, and between these statistical peaks; in particular, it is not unusual for single emissions to cross $f/f_H = 0.50$. When two bands are simultaneously present individual emission elements only rarely show one-to-one correlation between bands. For low K_p the median bandwidth of the upper band, gap and lower band are all ~16% of their centre frequencies, independent of L; for higher K_p the bandwidth of the lower band increases. Bandwidth also increases with latitude beyond ~10°. Starting frequencies of narrowband emissions range throughout the band. The majority of the emissions rise in frequency at a rate between 0.2 and 2.0 kHz/sec; this rate increases with K_p and decreases with L. Falling tones are rarely observed at dipole latitudes <2.5°. The observations are interpreted in terms of whistler-mode propagation theory and a gyroresonant feedback interaction model. An exact expression is derived for the critical frequency, $f/f_H \cong 0.5$, at which the curvature of the refractive index surface vanishes at zero wave normal angle. Near this frequency rays with initial wave normal angles between 0° and −20° are focused along the initial field line for thousands of km, enhancing the phase-bunching of incoming gyroresonant electrons. The upper peak in the bimodal normalized frequency distribution is attributed to this enhancement near the critical frequency, at latitudes of ~5°. Slightly below the critical frequency interference between modes with different ray velocities may contribute to the dip in the bimodal distribution. The lower peak may reflect a corresponding peak in the resonant electron distribution, or guiding in field-aligned density irregularities. The observations are consistent with gyroresonant generation of emissions near the equator, followed by spreading of the radiation over a range of L shells farther down the field lines.

1. INTRODUCTION

Wave–particle interactions are believed to play a fundamental role in the physics of the outer magnetosphere, controlling the structure and stability of the radiation belts. It is not surprising therefore that a number of theories of whistler-mode wave-particle interactions in this region have been advanced (Kennel and Petscheck, 1966; Helliwell, 1967, 1970; Sudan and Ott, 1971; Dysthe, 1971; Nunn, 1971, 1974; Brinca, 1972a,b; Helliwell and Crystal, 1973). Much of this theoretical work is based on an inadequate knowledge of the characteristics of whistler-mode VLF noise actually observed in this region. A primary aim of the present report is to provide a statistically accurate description of the most typical form of VLF radiation beyond the plasmapause: bandlimited chorus. A second aim is to interpret certain aspects of the frequency distribution of chorus in terms of a gyroresonant electron feedback model of generation (Brice, 1964; Helliwell, 1967). It is shown how a change in curvature of the whistler-mode refractive index surface will affect focusing of radiation along magnetic field lines, and how interference can occur between modes with slightly different ray velocities. Amplitudes and growth rates of magnetospheric chorus are discussed in a separate paper (Burtis and Helliwell, 1975).

Chorus measurements were made with the Stanford University/Stanford Research Institute broadband VLF (0.3–12.5 kHz) receiver on OGO 3. The VLF experiment package is similar to that flown on

OGO 1 as described in Dunckel and Helliwell (1969), except that the OGO 3 antenna can be connected through a matching transformer either as an electric field sensor or as a magnetic loop. A complete description of the instrumentation is given by Ficklin *et al.* (1967). OGO 3 maintained three-axis stabilization about the z axis with a period of ~100 sec. Initial perigee was less than 500 km altitude, apogee was over 120,000 km, inclination was 31°, and period was 48.5 hr. During the next 12 months the orbit inclination gradually increased to ~50°.

Virtually all passes from 15 June 1966 (VLF antenna deployment) to 14 June 1967 that were acquired with good telemetry were spectrum analyzed inside $L=8$ (often inside $L=10$). Spectrum analysis was performed with a Raytheon Rayspan analyzer over the range 0–10 kHz, except that when the electron gyrofrequency dropped to less than 5 or 2.5 kHz the range of spectral analysis was correspondingly reduced to 0–5 or 0–2.5 kHz. This insured that all whistlermode activity from 0.3 to 10.0 kHz would be analyzed with the best possible resolution. On those rare occasions when chorus activity extended above 10 kHz the analysis range was increased to 0–12.5 kHz. Frequency resolution was 1% of the analysis range, e.g. 100 Hz in the case of a 0–10 kHz record. (All of the spectrograms illustrating this report, in contrast to the routine data, were made with a Federal Scientific Ubiquitous UA6BH analyzer.)

Over 400 hrs of continuous broadband data were thus available for study. Because chorus activity was generally similar from minute to minute, it was possible to reduce the data analysis burden by measuring only every fifth minute of data. The satellite velocity at $L=6$ near the equator was ~4 km/sec; thus the satellite moved 0.2 R_E from one sample to the next. Occasionally at large distances (where the velocity was lower) the sampling interval was increased to 10 min. A total of 4,668 data samples was obtained.

Data coverage as a function of dipole latitude, L, and local time is shown in Fig. 1. Sample locations have been projected longitudinally onto either the noon–midnight or the dawn–dusk meridional plane, whichever is closer (e.g. dawn includes 0300–0900 LT). Each integer indicates the number of samples at that location. Dipole field lines are drawn for $L=4$, 7 and 10. In these plots a data gap is apparent at low L values on the equator and at northern midlatitudes. This is due entirely to the characteristics of the OGO 3 orbit, with locations south of the gap corresponding to inbound passes, and locations north of the gap to outbound passes. The equatorial data coverage is good for the midnight and dusk quadrants, but becomes progressively worse in the noon and dawn quadrants as the orbit inclination increases. In the dawn quadrant there are no data within 7° of the dipole equator for $2<L<6$. However, the dawn equatorial region from $L=4$ to 6 was well covered by OGO 1 (Burtis, 1969).

2. DEFINITION AND OCCURRENCE

For the purpose of this study, any discrete noise appearing on the spectrograms, regardless of its frequency, was considered to be chorus. The term "discrete" implies structured emissions having amplitude and/or frequency modulation with durations typically on the order of 0.1–1.0 sec. An important advantage of continuous broadband data over more compressed data formats is that it permits discrete emissions to be distinguished from unstructured hiss and whistlers.

Attention was focused on discrete structured activity in this study for two reasons. First, the most common phenomenon observed in the outer magnetosphere by the OGO 3 broadband VLF experiment was in fact discrete, choruslike activity. Second, unstructured hiss is often difficult to distinguish from background noise, and the upper and lower cutoffs of weak bandlimited hiss are very difficult to measure objectively using the broadband records. However, it should be borne in mind that chorus was often accompanied by a background of hiss having a variable amount of structure. The hiss was at times quite strong and occasionally appeared without any apparent chorus accompaniment. In a previous study based on OGO 1 and some OGO 3 data (Burtis, 1969), this unstructured noise was called "banded hiss" because of its tendency to accompany bandlimited chorus. Its region of maximum occurrence was found to be generally similar to that of "banded chorus" (and to the region of occurrence of chorus described in the present paper). It was observed somewhat less frequently than chorus in the dawn and noon quadrants but during the rest of the day the two types of noise occurred with roughly equal probability. A second and distinct class of unstructured noise, called ELF hiss, is commonly seen at lower normalized frequencies (wave frequency/gyrofrequency) inside the plasmapause (Gurnett and O'Brien, 1964; Burtis, 1969; Dunckel and Helliwell, 1969; Russell *et al.*, 1969; Muzzio and Angerami, 1972). Plasmaspheric ELF hiss is usually not accompanied by discrete chorus activity.

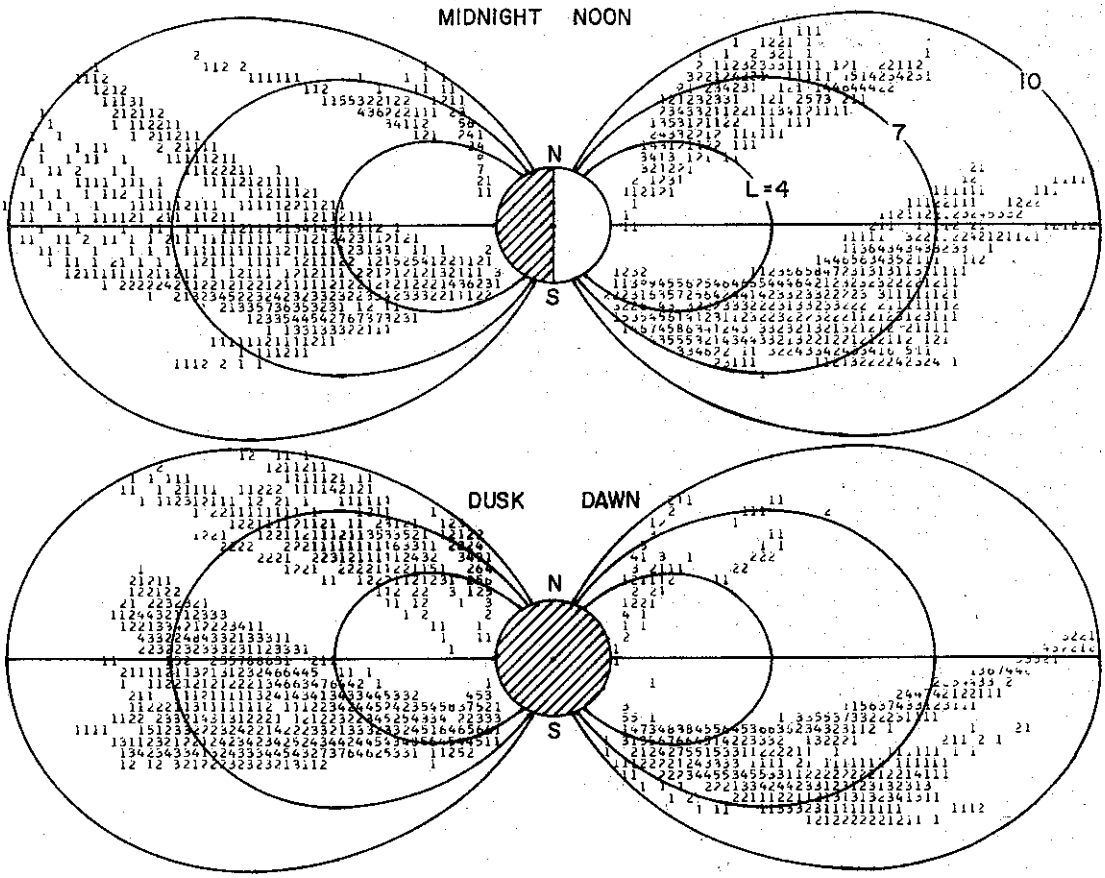

FIG. 1. DATA COVERAGE PROJECTED ONTO THE NOON–MIDNIGHT AND DAWN–DUSK MERIDIONAL PLANES.

Computer-printed integers indicate the number of samples taken at that L value and dipole latitude, for each of four six-hour local time quadrants.

It should be emphasized that the term "banded chorus" was introduced to describe the bandlimited nature of the ensemble of magnetospheric chorus elements (Burtis and Helliwell, 1969). The term does not apply to the closely spaced, constant frequency striations of individual chorus elements ("single modes") later reported by Coroniti *et al.* (1971). Nunn (1974) has developed a theory attempting to account for such mode structure in the generation of chorus. However, Stiles (1975) has suggested that these apparent single modes may be an artifact of the analysis procedure in which closely spaced rising or falling tones are transformed into horizontal bands. Thus the reality of single modes is not definitely established. In the present work no positive evidence of single modes has been found. It should be noted that some of the illustrations in this paper, which may appear to show single modes (e.g. Fig. 2d), were made with a relatively coarse time resolution; none of these apparent single modes was found to persist longer than the response time of the analyzer. To avoid confusion over the word "banded," its use has been dropped in favour of the general term "magnetospheric chorus" in the present work.

An example of high chorus activity found in the OGO 3 pass of 25 August 1966 is illustrated in Fig. 2. The satellite was outbound in the noon quadrant (13–15 LT) at a nearly constant dipole latitude of 25°. Geomagnetic activity was moderate; K_p was currently 2 but had reached 4 some 12 hr earlier. The antenna was in the magnetic mode. A band of chorus and hiss moving down in frequency from over 3 kHz at $L=4.5$ to less than 1 kHz at $L=8.5$ is shown at the top. Since the time scale is very compressed in this top spectrogram (nearly two

hours of data are shown), the individual emissions comprising the chorus band are not readily discernable. Perturbations in the regular decrease in frequency (e.g. at ~0317 and ~0411 UT) may be evidence of partial ducting due to electron concentration gradients. The noise below 1 kHz prior to 0300 UT is ELF hiss, and contains no discrete emissions. Vertical striations in the background noise are due to telemetry fading at the satellite spin period of ~100 sec. A calibration signal at 1 kHz and harmonics is seen every 4.9 min. In addition there is a faint interference line at the satellite inverter frequency of 2.46 kHz; the frequency increase in this line at ~0240 and 0333 UT is an artifact due to tape speed slow downs in the original NASA recordings. Power line harmonics at 120 and 240 Hz, introduced at the ground station, may be seen at the bottom of the record. There is evidence of the third harmonic of the strong chorus band after 0320 UT, which is caused by the nonlinear response of the logarithmic amplifier. The GSFC Rb vapour magnetometer experiment was turned off during this pass, so no magnetometer line appears on the records.

Selected 60 sec samples from this pass are shown in Figs. 2(b–e). The time scale has been expanded by a factor of 100 so that the individual emissions can be seen, and the frequency range of analysis has been adjusted to improve the resolution. Frequency (df) and time (dt) resolution depend on the frequency range of the Ubiquitous spectrum analyzer and are given in the text for each example. In part b($df = 10$ Hz, $dt = 100$ ms) the chorus emissions at ~3 kHz are intermittent and are not accompanied by hiss. The ELF hiss below 1 kHz is attenuated by the receiver AGC during strong chorus emissions. A telemetry fade occurs at ~7 sec from the start of the record. The chorus emissions are not well developed; some consist of very short falling or rising elements, while others are brief, amorphous "dots." Note that the chorus bandwidth is small.

A time at which the noise band is composed mainly of hiss with weak internal structure is illustrated in part c ($df = 5$ Hz, $dt = 200$ ms). Occasional strong "hooks" emerge from the hiss; the middle hook at 33 sec appears to trigger two secondary hooks at a somewhat higher frequency.

Typical chorus mixed with a background of hiss is shown in Fig. 2(d) ($df = 2.5$ Hz, $dt = 400$ msec). Most of the emissions are rising tones or hooks, which appear to begin throughout the lower half of the band. The relative bandwidth of the chorus is much larger in this case than for panel b. Note that the horizontal striations in any one emission do not appear to persist longer than the 0.4 sec time resolution, suggesting that they correspond to amplitude modulation of a single gliding tone rather than to several constant frequency "single modes."

Finally, part e ($df = 2.5$ Hz, $dt = 400$ msec) shows chorus at $L = 9$, LT = 1510, which appears intermittently about 10 min beyond the end of the top panel. Although the nominal lower cutoff frequency of the broadband VLF receiver is 300 Hz,

FIG. 2. HIGH CHORUS ACTIVITY DURING AN OUTBOUND PASS THROUGH THE NOON MAGNETOSPHERE NEAR 25° DIPOLE LATITUDE.

Top panel: compressed spectrogram showing decrease in frequency of chorus band. Panel b: intermittent short chorus emissions (~3 kHz) above ELF hiss (<1 kHz). Panel c: bandlimited hiss and occasional chorus emissions. Panel d: typical chorus with background hiss. Panel e: chorus emissions starting below 200 Hz at dipole $L = 9$.

FIG. 3. MAGNIFIED SPECTRUM SHOWING COMPLEXITY OF CHORUS EMISSIONS OBSERVED AT $L = 7.8$, 40° DIPOLE LATITUDE, 1210 LT.

Rising tones, falling tones, and hooks all are present in the chorus; some appear to be triggered by previous emissions while others arise spontaneously from the background hiss.

FIG. 7. EQUATORIAL CHORUS DETECTED WITH THE ELECTRIC ANTENNA; DIPOLE COORDINATES OF THE SATELLITE ARE SHOWN.

Top panel: compressed spectrum showing double band of chorus increasing in frequency (magnetometer lines inserted at $f_H/4$ and harmonics). Panel b ($\lambda = 0°$): arrow indicates 0.50 f_H; note absence of chorus between 0.45 and 0.55 f_H. Panel c ($\lambda = -2°$): note low correlation of emissions between upper and lower band. Panel d ($\lambda = -5°$): here there is an unusual degree of correlation between bands; the upper band now begins near $f/f_H = 0.49$.

FIG. 8. EQUATORIAL CHORUS DETECTED WITH THE MAGNETIC ANTENNA.

Panel a: double band of chorus, with upper band starting just below 0.5 f_H. Panel b: less typical single chorus band with emissions crossing 0.5 f_H. Panel c: double band of chorus, with upper band (~0.55 f_H) very narrow and uncorrelated with lower band.

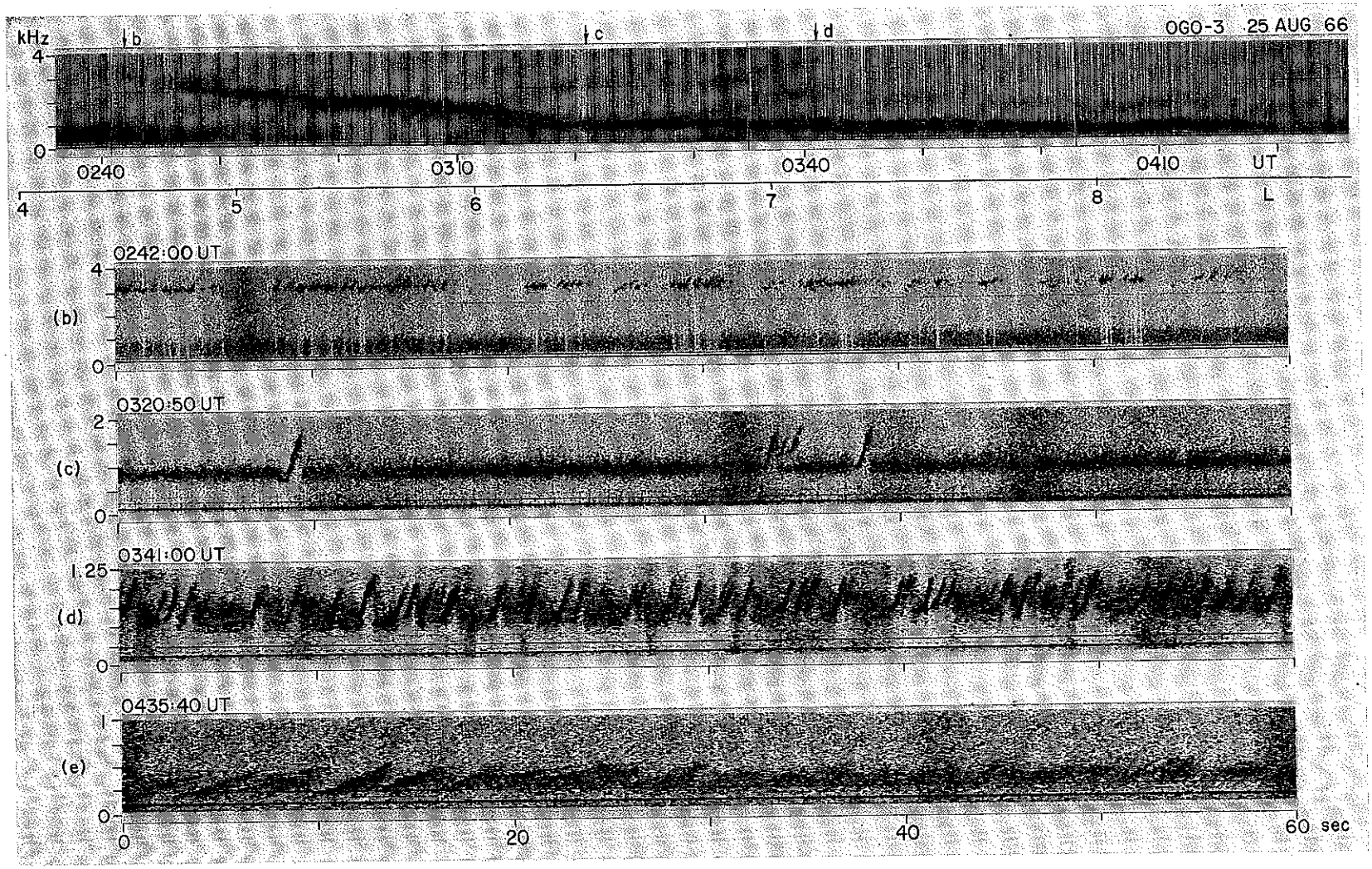
kHz
4
0
b
c
d
OGO-3 25 AUG 66
0240
0310
0340
0410
UT
4
5
6
7
8
L
0242:00 UT
(b)
0320:50 UT
(c)
0341:00 UT
(d)
0435:40 UT
(e)
0
20
40
60 sec

FIG. 2

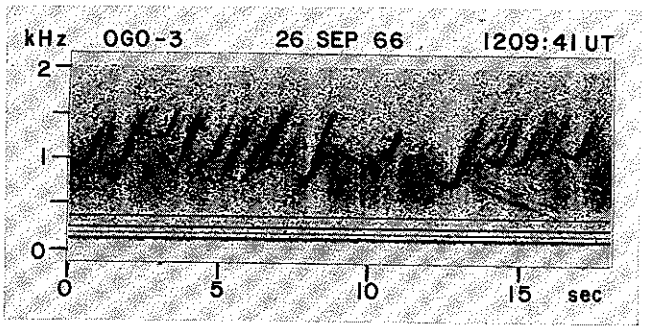

FIG. 3

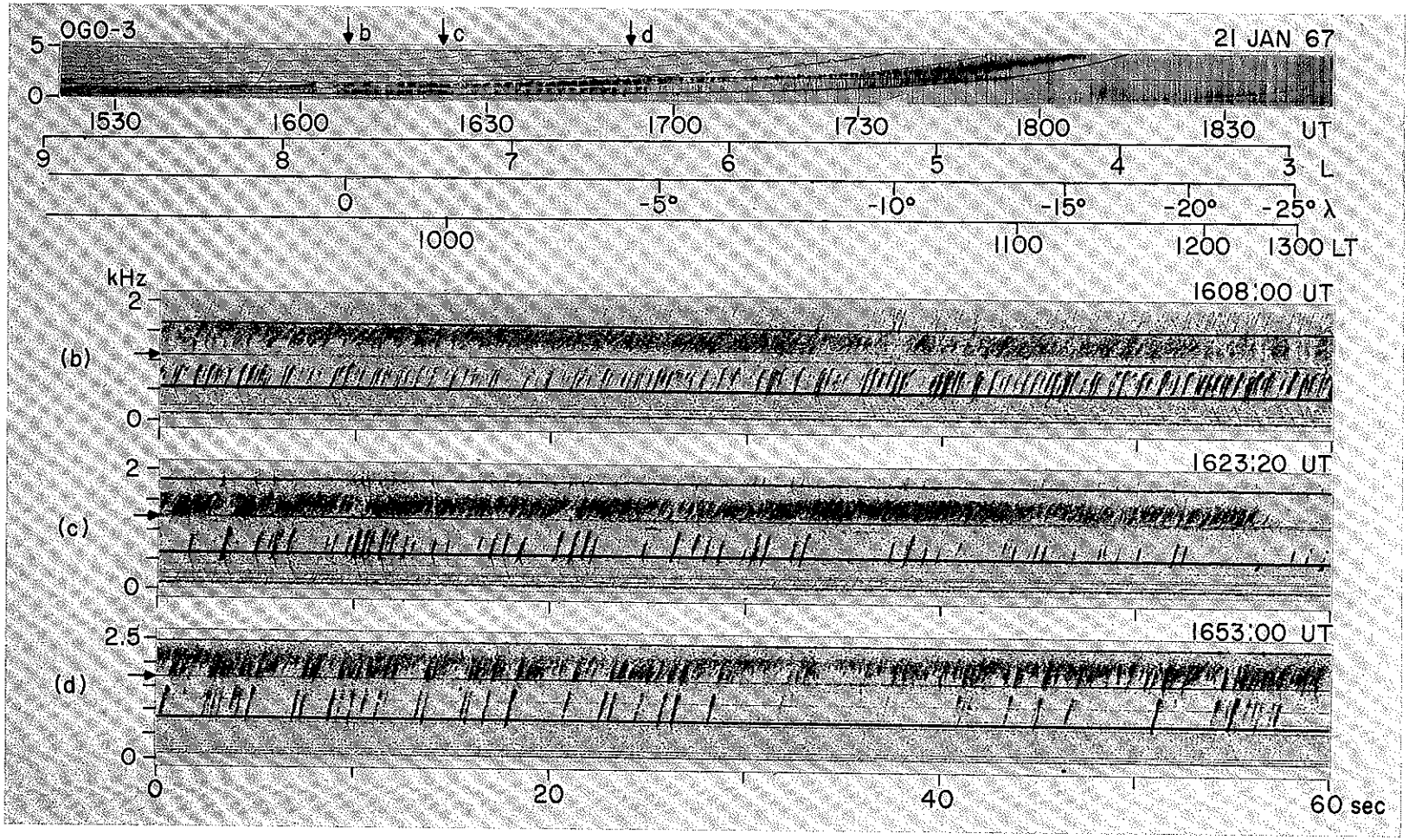
OGO-3
b
c
d
21 JAN 67
5
0
1530
1600
1630
1700
1730
1800
1830
UT
9
8
7
6
5
4
3
L
0
-5°
-10°
-15°
-20°
-25° λ
1000
1100
1200
1300 LT
kHz
1608:00 UT
(b)
2
0
1623:20 UT
(c)
2
0
1653:00 UT
(d)
2.5
0
0
20
40
60 sec

FIG. 7

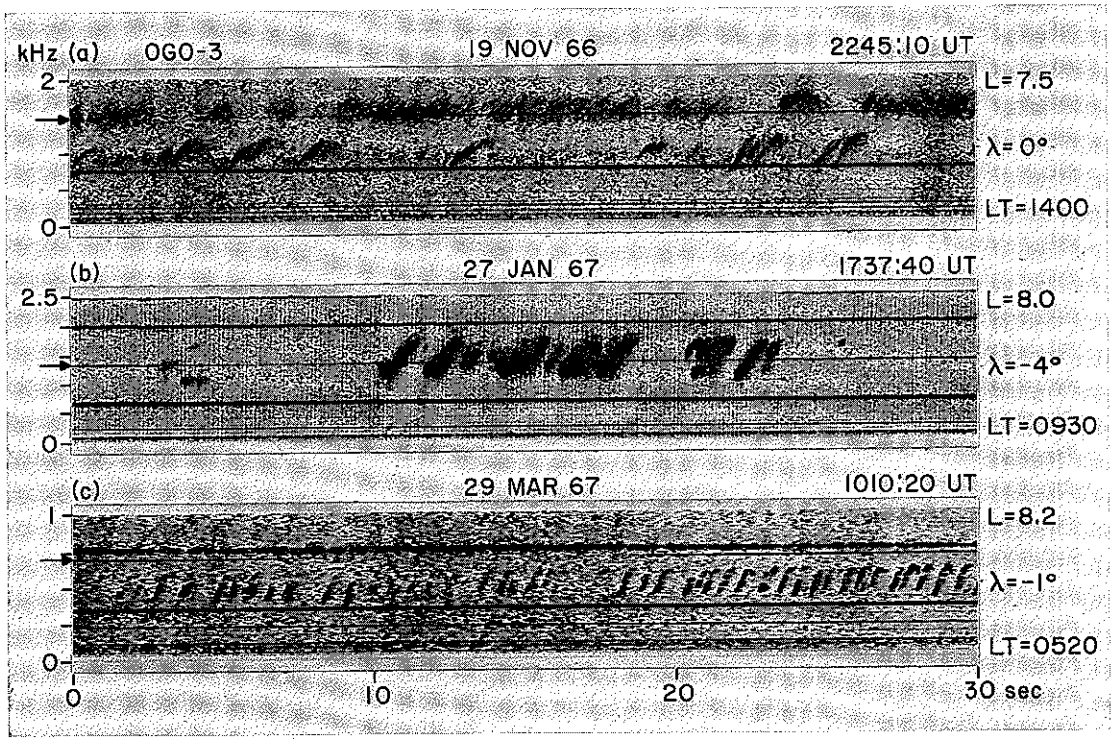
kHz (a) OGO-3
19 NOV 66
2245:10 UT
2
0
L=7.5
λ=0°
LT=1400
(b)
27 JAN 67
1737:40 UT
2.5
0
L=8.0
λ=-4°
LT=0930
(c)
29 MAR 67
1010:20 UT
1
0
L=8.2
λ=-1°
LT=0520
0
10
20
30 sec

FIG. 8

rising emissions may be seen at least as low as 200 Hz in this example. There seems to be no interaction with the 240 Hz power line harmonic, which is believed to be an artifact introduced at the telemetry receiving station. The weak third harmonic distortion of the strong emissions between 10 and 20 sec is also an artifact. There is some suggestion of a ~3 sec periodicity in the emissions; whistler-mode echoing is an unlikely explanation since the two-hop period is estimated to be ~14 sec.

In each of these 60 sec samples the chorus is quite sharply bandlimited. No discrete emissions were observed at frequencies either above or below the illustrated band. The occurrence and spectral properties of the chorus elements are relatively constant during the 60 sec intervals, but may change markedly over a period of 20 min. As described elsewhere, in the statistical analysis a 60 sec sample was scaled every 5 min.

The spectral complexity of some magnetospheric chorus is illustrated by the enlarged spectrum of Fig. 3. OGO 3 was at $L = 7.8$, +38° dipole latitude, 1210 local time; geomagnetic activity was moderate ($K_p = 4$); and the antenna was in the magnetic mode. Frequency resolution $df = 5$ Hz, time resolution $dt = 200$ msec. Power line interference is seen at 120, 240 and 360 Hz. Receiver AGC attenuation of the background noise caused by strong emissions is especially pronounced at ~8 and ~13 sec. Chorus activity similar to this was seen for many minutes before and after the 18 sec sample shown. Rising tones, falling tones, and hooks all may be observed in the mix of emissions constituting the chorus band. Some emissions appear to be triggered by previous emissions, while others appear to arise spontaneously from the background hiss. No whistlers are in evidence; whistlers are rarely apparent in magnetospheric chorus (occasionally they are seen near the inner boundary of chorus activity, probably near the plasmapause).

To obtain the statistical results presented in this report, an objectively chosen 60 sec interval of each 5 min of data was intensely scrutinized and various parameters were measured. If any discrete noise at any frequency appeared during the 60 sec interval, chorus was said to have occurred. Of the total of 4668 data samples, chorus occurred in 1251 (27%). The remaining 73% showed either no signals or just hiss or whistlers. Occurrence of chorus was essentially independent of whether the antenna was connected in the electric or magnetic mode, suggesting that the bulk of the discrete emission activity was electromagnetic in character.

Chorus occurrence depended strongly on local time. A pronounced increase near 0300 and a decrease near 1500 divided the active morning-dayside region, where occurrence averaged nearly 50%, from the quiet evening-nightside region, where occurrence averaged only 12%. Tsurutani and Smith (1974) have reported a sudden onset of chorus below 1500 Hz at local midnight with a sharp peak at 0100 LT (called by them "postmidnight chorus"). They also state that "no chorus was seen in the 3 hr preceding midnight." This latter finding is difficult to reconcile with the present study, in which at least occasional chorus was seen in virtually all regions of the magnetosphere; perhaps this reflects a difference in the definition of chorus occurrence. The present study shows some gradual increase in occurrence from 2100 to 0100, but no sudden onset at midnight and no sharp postmidnight peak.

Chorus occurrence projected along dipole field lines onto the equatorial plane is shown in Fig. 4. Heavy shading indicates occurrence >50%, while light shading indicates 21–50%. Data coverage was inadequate beyond the peripheral boundaries. An outward spiral of maximum chorus is evident, from L ~3 to 6 predawn to L ~5 to 9 postnoon (the anomalously low occurrence for $4 < L < 6$, $07 < \mathrm{LT} < 08$ is attributed to the fact that on the average geomagnetic activity was lower here than for any other region). Since chorus from all dipole latitudes is included in Fig. 4, and since high latitude chorus has in general propagated to slightly lower L values (Burtis and Helliwell, 1969), the location of maximum chorus generation in the equatorial plane may be at slightly higher L than shown; however, the correction is estimated to be less than 0.5 L. A dashed curve, linear in L vs LT, roughly traces the locus of maximum chorus occurrence in Fig. 4. The spiral is reminiscent of, but at lower L values than, such well studied magnetospheric boundaries as the limit of closed field lines or the 40 keV electron trapping limit (Burrows and McDiarmid, 1972). The general region of maximum occurrence approximates the zone of "hard" electron precipitation reported by Hartz and Brice (1967). However, these authors state that the invariant latitude (~65°, corresponding to dipole $L = 5.6$) of the morning maximum of hard electron precipitation is essentially independent of local time, not showing the spiral characteristic of higher latitude geophysical phenomena. This difference might be explained by the decrease in wave frequency with L that is characteristic of chorus. For a typical electron density model, the parallel resonant energy of the

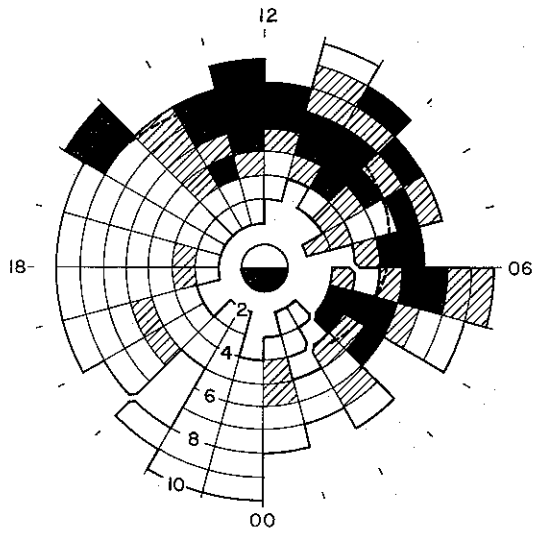

FIG. 4. DIURNAL VARIATION OF CHORUS OCCURRENCE, PROJECTED ALONG DIPOLE FIELD LINES ONTO THE EQUATORIAL PLANE.

Light shading indicates 21–50% occurrence; heavy shading indicates over 50% occurrence. Dashed line shows gradual outward spiral of region of maximum occurrence.

interacting electrons decreases roughly as L^{-3} (Helliwell, 1970). Thus the noon chorus at high L values would tend to precipitate softer electrons. However as Fig. 4 shows, the level of chorus activity in the region $5<L<6$ shows little variation from 0300 to 1500 LT, in rough agreement with the region of hard electron precipitation (Hartz and Brice, 1967).

This diurnal variation of chorus occurrence is reasonably similar to that of chorus observed at ground stations, and is consistent with peak chorus activity occurring later in the day at higher latitude stations (Storey, 1953; Allcock, 1957; Pope, 1963; Laaspere *et al.*, 1964). It seems to be consistent with the occurrence reported by Taylor and Gurnett (1968) of undifferentiated ELF hiss and VLF chorus on Injun 3 at low altitudes, if it is assumed that most of their activity after 1600 LT is ELF hiss. It is also consistent with the occurrence of ELF "noise bursts" at $L>7$ (Russell *et al.*, 1969) when the 1000 Hz upper frequency cutoff of their instrument is taken into account. The diurnal variation is in good agreement with an earlier study on the occurrence of banded chorus (Burtis, 1969), which was based in part on a limited subset of the present OGO 3 data and in part (especially in the dawn quadrant) on OGO 1 data. The low intensity of chorus over much of this region in the study by Dunckel and Helliwell (1969) is attributed to low geomagnetic activity (see below).

The range of L values over which chorus was observed on a given pass was extremely variable. Tsurutani and Smith (1974) reported "chorus emissions, when detected, were found over a range of L shells, the extent of which was greater than 2 but less than 4 R_E." In the present study, ranges of less than 2 R_E were very common, and ranges greater than 4 R_E were occasionally observed. For example, on the inbound pass of July 9, 1966 through the midnight region chorus was seen continuously from $L=8$ to 3, and on 21 January 1967 in the noon quadrant chorus occurred throughout the region from $L=10$ to 4 (Fig. 7).

Chorus occurrence was also found to depend strongly on dipole latitude. Including data for all L and LT, percentage occurrence was moderate (~27%) within 10° of the dipole equator, declined to a minimum (~17%) near 15°, and then increased gradually to high levels (~44%) at high latitudes, far down the field lines. Occurrence was somewhat higher at 5° than at the dipole equator, but the significance of this is uncertain. The reason is that much of the equatorial data comes from high L values where the location of the magnetic equator (minimum in magnetic field strength along field line) differs from the dipole model due to tilt of the geomagnetic axis with respect to the Earth–Sun line. However other evidence is presented below for generation of chorus at latitudes near 5°. Away from the near equatorial generation region occurrence decreases, presumably due to attenuation, but beyond ~15° occurrence again increases. This may be caused both by convergence of field lines and by spreading of the radiation over a range of field lines so that multiple equatorial source regions are viewed simultaneously. Alternatively some emissions may be generated far down the field lines, but investigation of the normalized frequency (see below) makes this interpretation seem less likely.

Russell *et al.* (1969) reported steadily decreasing occurrence of ELF "noise bursts" with increasing dipole latitude. However, they found strong peaks in "steady noise" at latitudes around 45° at $L>6$ on the dayside. Since chorus occurrence was found to be very high in this high latitude region in the present study, it is suggested that these peaks in "steady noise" may have been caused by saturation of their instrument by closely spaced chorus emissions. This is consistent with the frequent occurrence of chorus somewhat farther down the field lines at altitudes of 250 to 2000 km (Gurnett and

O'Brien, 1964; Taylor and Gurnett, 1968). Tsurutani and Smith (1974) found "postmidnight chorus occurred only within ±15° of, and most frequently at, the geomagnetic equator." In the present study, chorus was seen in the midnight quadrant at all dipole latitudes to 50°. It is suggested that the OGO 5 orbit may be partly responsible for the results of the Tsurutani and Smith (1974) study. For example, Burton and Holzer (1974) state that on 14 August 1968, OGO 5 traveled "from 7.9 to 5.9 R_E as it went from $\lambda_m = 2.9°$ to $-4.2°$." At the latter position the electron gyrofrequency for the dipole field is ~4 kHz (on this pass it was measured at 2.6 kHz (Tsurutani and Smith, 1974)). To reach higher dipole latitudes on this type of orbit OGO 5 must travel to regions of higher magnetic field intensity. Since the upper cutoff of the UCLA fluxgate is nominally 1 kHz (Frandsen *et al.*, 1969; Burton and Holzer, 1974) it is likely that the frequency of most banded chorus would pass above the limit of their instrument by the time OGO 5 reached dipole latitudes of 15°. Indeed, Tsurutani and Smith (1974, Fig. 6) show the band of chorus already passing the 1000 Hz cutoff at the latter position (−4.2°) mentioned above.

Chorus occurrence was found to correlate more strongly with K_{pm}, the maximum value of K_p during the previous 24 hr, than with current K_p (Burtis, 1974). This suggests a time lag between particle injection on the nightside and the onset of chorus on the dayside. In addition, the inner boundary of chorus activity moved inward as geomagnetic activity increased. Using the arbitrary figure of 20% occurrence, the inner boundary moved from $L = 5.5$ for $0 \leq K_{pm} \leq 1$, to $L = 2.6$ for $6 \leq K_{pm} \leq 9$. Carpenter (1967) found a similar inverse correlation between K_{pm} and the distance of the plasmapause at dawn. This is further evidence that chorus is primarily of extra-plasmaspheric origin. The inward movement is consistent with ground observations (Helliwell, 1960; Crouchley and Brice, 1960) and low altitude satellite observations (Taylor and Gurnett, 1968) showing an equatorward movement of chorus activity during geomagnetically disturbed periods. Dunckel and Helliwell (1969) observed the most intense chorus on OGO 1 at quite large distances (L ~9). Two reasons are suggested for this result. First, geomagnetic conditions were significantly more quiet during their period of observations (average $K_p = 1.5$) than during the present study (average $K_p = 2.0$). Second, there is evidence that chorus intensity is negatively correlated with frequency, and hence positively correlated with L (Burtis and Helliwell, 1975).

The individual discrete emissions comprising chorus sometimes appeared as short, amorphous noise bursts, but usually could be described as rising, constant, or falling in frequency, or of the compound U-shaped form called hooks (Gallet, 1959). More accurately, "constant frequency" tones in the present study refer to narrowband emissions whose slopes were not resolved on the routine spectrograms, i.e. $|df/dt| < 0.1$ kHz/sec. Often several spectral forms were observed in the same sample, although one form usually was predominant. Each of these spectral forms was observed at least occasionally in all regions of the magnetosphere, day and night, high and low L, equatorial and high latitude, geomagnetically active or quiet. Overall, rising tones were most common, being observed in 77% of the samples, followed by falling tones (16%), constant frequency tones (12%) and hooks (6%). The percentage for hooks, based on routine spectrograms, may be somewhat low; with higher resolution many rising tones appear to begin with a small hook. Burton and Holzer (1974), in an OGO 5 study of chorus below 1000 Hz, found "dayside chorus consisted solely of rising tones." This was not true in the present study; although rising tones did have above average occurrence (85%) in the noon quadrant, other spectral forms were also observed.

Very few samples in the equatorial region, from −2.5° to +2.5° dipole latitude, included any falling tones. Yet just off the equator, from ±2.5° to ±10.5°, there was an increase in occurrence of falling tones (Table 1). At higher latitudes occurrence of falling tones was somewhat lower and fairly constant. The majority of near equatorial samples come from high L, and there may be considerable distortion of the dipole field, including a shift in location of the equator due to tilt of the dipole axis.

TABLE 1. NUMBER OF SAMPLES NEAR THE EQUATOR THAT INCLUDED RISING AND FALLING TONES

Dipole latitude range	Rising (R)	Falling (F)	Ratio (R/F)
−10.5°–−2.5°	149	71	2.10
−2.5°–+2.5°	71	7	10.13
+2.5°–+10.5°	45	11	4.09

This may account for the 7 samples having falling tones within 2.5° of the dipole equator. All 7 are from geomagnetically active periods with $K_{pm} \geq 4$. This, together with the observation of an increased occurrence of falling tones both to the north and to the south of the dipole equator, gives support to models (e.g. Helliwell 1967, 1970) in which falling tones travel away from the equator as they leave the generation region (see Fig. 13 below). On the other hand, we have no good explanation for a similar decrease in falling tone occurrence near −20°.

The mix of emissions in a given chorus sample usually included a predominant spectral form with a fairly constant slope, *df/dt*. Whenever practical, this "typical" slope was measured as approximating one of 12 discrete, quasi-logarithmically spaced values from 0.1 to 70.0 kHz/sec, or zero. Rising tones were predominant in the majority (84%) of the 1032 samples in which the measurement was made. Based on logarithmic interpolation between measured values, the median *df/dt* for the 867 samples of rising tones was 0.77 kHz/sec. Of these samples 50% had slopes between 0.38 and 1.44 kHz/sec.

Variation of the median slope of rising tones with location and geomagnetic activity is shown in Fig. 5. In each case the solid line indicates the variation in median slope for the entire data set, vertical bars indicate the 50% range for the entire data set, and dashed lines indicate the variation in median slope for subsets of the data set. Figure 5(a) shows a diurnal decrease in slope, with the highest slopes in the midnight quadrant. This may be related to the outward spiral of chorus occurrence (Fig. 4), since Fig. 5(b) shows a strong negative correlation between slope and L value. The upper dashed curve in Fig. 5(a) is for the subset of data having $4 \leq L \leq 6$, while the lower dashed curve is for $6 \leq L \leq 8$. Although no consistent diurnal variation in slope is seen for constant L, there does seem to be a diurnal decrease for $4 \leq L \leq 6$; however the sample size in the midnight quadrant is small. Figure 5(b) shows a very regular decrease in slope with increasing L value. For the entire data set (solid line) *df/dt* varies as L^{-2}. However, the dashed line shows a steeper decrease in slope for the subset of data within 10° of the dipole equator, i.e. close to the generation region. Figure 5(c) shows no consistent variation in slope with dipole latitude (the upper dashed curve is for $4 \leq L \leq 6$, the lower dashed curve is for $6 \leq L \leq 8$). Since most emissions are fairly close to the whistler nose frequency, the one-half hop dispersion will be small. Finally, Fig. 5(d) shows a pronounced increase in slope with increasing geomagnetic activity (again the upper dashed curve is for $4 \leq L \leq 6$, the lower dashed curve is for $6 \leq L < 8$). A similar correlation of chorus *df/dt* with magnetic activity has been reported at a ground station (Allcock and Mountjoy, 1970). The L and K_{pm} variation (Figs. 5b,d) are not completely independent since the region of chorus occurrence moves inward during geomagnetically active periods. However, the dashed curves of Fig. 5(d) imply that *df/dt* increases with K_p even at constant L, and it was also found that *df/dt* decreases with L even at constant K_p.

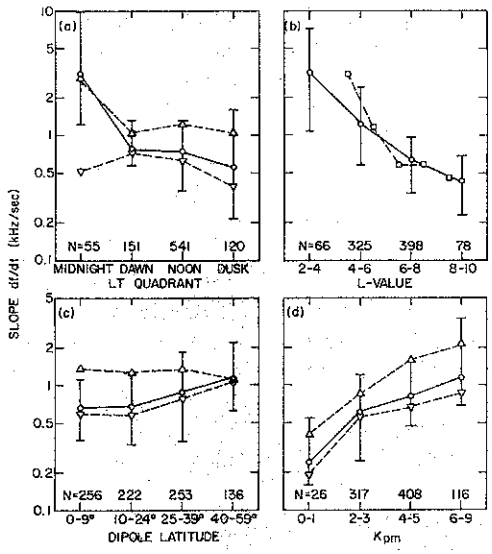

FIG. 5. VARIATION IN RATE OF FREQUENCY CHANGE OF RISING TONES.

Solid curves show median *df/dt* for entire data set, vertical bars indicate range of variation of 50% of entire data set, and dashed curves show median *df/dt* for following subsets: squares (b), $\lambda < 10°$; upper triangles (a, c, d), $4 \leq L < 6$; lower triangles (a, c, d), $6 \leq L < 8$.

3. CHORUS FREQUENCY

Magnetospheric chorus usually occurs in rather well defined bands whose frequency varies with the location of the satellite (Burtis and Helliwell, 1969). More than one band may be present at a given time. In the present study, if discrete emissions were present during a 60 sec sample, they were grouped according to band (generally a straightforward, obvious procedure) and four frequencies were scaled for each band. Two of the frequencies were simply the lower (f_L) and upper (f_U) cutoff of the band, i.e. the minimum frequency of any emission in the band, and the maximum

frequency of any (probably a different) emission in the band, during the 60 sec interval. The other two measured frequencies were the minimum (f_{sL}) and maximum (f_{sU}) starting frequency, i.e., the lowest and highest frequency at which any emissions appeared to begin during the 60 sec interval. By measuring the range of starting frequencies, it was hoped that more useful information could be gained regarding the generation process. It is well known from studies of artificially stimulated emissions (Helliwell *et al.*, 1964; Stiles and Helliwell, 1975) that a single triggering frequency can produce emissions extending over a considerable range of frequencies. However, in the present study it was usually found that the range of starting frequencies of a chorus band was only slightly less than the bandwidth. In a band of rising tones, for example, there were usually very short risers starting near the upper cutoff of the band.

Of the 1251 samples with chorus activity, 79% had only a single band of emissions, 20% two bands and 1% three or more bands, giving a total of 1516 bands of chorus. The occurrence of multiple bands was relatively independent of local time, L value, and magnetic activity, but was strongly correlated with dipole latitude. Within 9° of the dipole equator 41% of the samples had multiple bands while at mid-latitudes only about 10% had more than one band. At high latitudes the occurrence of multiple bands recovered to ~20%. Double banding in the equatorial region has been previously reported by Burtis and Helliwell (1971) and Tsurutani and Smith (1974), and is discussed extensively below.

Magnetospheric chorus exhibited a broad distribution of bandwidth. Ninety per cent of the 1516 bands had a range of starting frequencies ($f_{sU}-f_{sL}$) between 5 and 108% of the centre frequency ($f_{sU}+f_{sL}$)/2 of the band, half were between 15 and 57%, and the median range of starting frequencies was 32% (i.e., ±16% of the centre frequency). Variation of median bandwidth with location and geomagnetic activity is shown in Fig. 6. The lowest curve (triangles) represents the median range of starting frequencies ($f_{sU}-f_{sL}$) for individual bands. The middle curve (circles) gives the median bandwidth (f_U-f_L) for individual bands. The highest curve (squares) represents the median overall bandwidth ($f_{U\max}-_{L\min}$) for 60 sec *samples*, which may or may not include more than one band. Figure 6(a) shows that bandwidths were roughly independent of local time. Similarly, Fig. 6(b) shows that bandwidths (relative to the centre frequencies) varied little with L value. Since the centre frequency

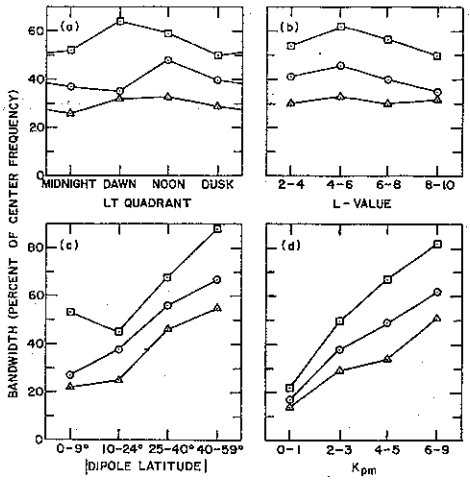

FIG. 6. VARIATION OF MEDIAN BANDWIDTH (CIRCLES), MEDIAN RANGE OF STARTING FREQUENCY (TRIANGLES), AND MEDIAN OVERALL BANDWIDTH OF ALL BANDS IN A SAMPLE (SQUARES).

Note that relative bandwidth is independent of local time or L value, but increases with dipole latitude and with geomagnetic activity.

varied roughly as L^{-3} (see below) this implies that *absolute* bandwidth also varied as L^{-3}, being ~27 times larger for $2<L<4$ than for $8<L<10$. A marked tendency for bandwidth to increase with dipole latitude is shown in Fig. 6(c). The relative median bandwidth of individual bands increased by a factor of ~2.5 from the equatorial region to high dipole latitudes (far down the field lines). Again this may be caused by spreading of radiation over a range of field lines so that multiple equatorial source regions are viewed simultaneously at high latitudes.

A very strong correlation of bandwidth with K_{pm} is shown in Fig. 6(d). Median bandwidth increased by a factor of ~3.5 from quiet to magnetically disturbed conditions. Allcock and Mountjoy (1970) have reported a similar, but somewhat less pronounced, correlation for chorus observed at a New Zealand ground station. The bandwidth of *equatorial* chorus also increased with magnetic activity, but in a rather interesting way. For the total of 141 observations of double bands within 9.5° of the dipole equator, the median range of starting frequencies of the lower band was 35% of the centre frequency of the lower band, the median range of starting frequencies of the upper band was 16% of the centre frequency of the upper band, and the median width of the gap between the bands was 16% of the centre frequency of the gap. As K_{pm} increased, the width of the gap and the upper band

remained relatively constant (13–19% of centre) while the width of the lower band increased from 13% of centre for $K_{pm}=0$–1, to 43% of centre for $K_{pm}=4$–5. Since the normalized frequency of the upper band and gap are independent of K_{pm} (see below), this implies that the lower band extended to lower normalized frequencies (gyroresonant with higher energy electrons) as geomagnetic activity increased.

The local electron gyrofrequency f_H was measured by the Goddard Space Flight Center Rb vapour magnetometer on OGO 3. This information was telemetered on the same link as the broadband VLF data, appearing on the spectrograms as lines at $f_H/4$ and harmonics. The value of f_H was scaled for each data sample whenever it was available (typically it varied by less than a few per cent over the 60 sec sample). A total of 861 cases of chorus bands with local gyrofrequency information was obtained.

Defining the frequency of a band of chorus as $f=(f_{sU}f_{sL})^{1/2}$, the normalized chorus frequency f/f_H was found to depend strongly on dipole latitude. In the equatorial region the normalized frequency distribution was quite narrow and had a double peak, as discussed below. Off the equator the distribution progressively broadened and there was no significant sharp peak. At mid to high latitudes the chorus frequency was much more closely related to the equatorial gyrofrequency f_{Ho} on the dipole field line passing through the satellite than to the local gyrofrequency, in agreement with previous studies (Dunckel and Helliwell, 1969; Burtis and Helliwell, 1969). These features imply that most chorus is generated near the dipole equator.

An example of chorus observed near the equatorial generation region is provided by the inbound OGO 3 pass on 21 January 1967, illustrated in Fig. 7. Chorus was detected with the electric antenna from $L=10.0$ to $L=4.1$ as the satellite travelled Earthward during the pre-noon hours (L value, dipole latitude, and local time coordinates are indicated in the figure). Geomagnetic activity was moderate: K_p was currently 2 and had reached 4 about 24 hr earlier. Over 3 hr of compressed data are shown at the top of Fig. 7. The chorus appears in two intermittent, closely spaced bands below 1 kHz at 1530 UT, and gradually increases in frequency to ~5 kHz at 1800 UT. No discrete chorus emissions are observed (even at frequencies higher than the range illustrated) after 1808 UT. Shortly after this time a lower hybrid resonance (LHR) noise band begins to appear at the geometric mean gyrofrequency, indicating a relatively dense plasma probably inside the plasmapause (Burtis, 1973, Fig. 5). The LHR appears as the sharp lower cutoff of a noise band increasing in frequency from ~0.4 to 2 kHz; there is also some ELF hiss with an upper cutoff of ~0.5 kHz below the LHR band. In addition to these emission bands, the GSFC magnetometer has been inserted in the spectrum at $f_H/4$ and harmonics (the fundamental goes off-scale at 1815 UT). At the beginning of the record at least ten harmonics may be seen, and these are frequency modulated at the satellite spin period (~100 sec) with a peak-to-peak frequency deviation of ~4%, suggesting a spacecraft magnetic field of ~1.4 milliteslas (in addition a magnetometer calibration appears every five minutes). The chorus (and associated hiss) shows some spin-periodic amplitude modulation (especially evident in the upper band between 1700 and 1730 UT), but no frequency modulation is apparent. Note that the chorus bands remain bounded by the fundamental and third harmonic of the magnetometer line ($0.25\ f_H<f<0.75\ f_H$). After about 1730 UT (beyond 9° latitude) the upper band drops below $f_H/2$ and the two bands tend to merge.

Selected 60 sec examples of near equatorial chorus observed on this pass are shown in Figs. 7(b–d). The time scale has been expanded by a factor of ~200, and the frequency range has been adjusted to best display the chorus bands (frequency resolution $df=5$ Hz). The arrow on the frequency scale indicates the second harmonic of the GSFC magnetometer, which equals one-half the local electron gyrofrequency ($f_H/2$). There is some harmonic distortion in these records, so that strong emissions may appear weakly at their third harmonic or may intermodulate with the magnetometer line and be "reflected" below it. There are also some interference lines caused by modulation products of the magnetometer line with satellite inverter lines and with power line harmonics of 120, 180 and 240 Hz.

Chorus observed at 0° dipole latitude is shown in Fig. 7(b). An upper band of chorus is seen from ~0.55 to ~0.75 f_H. A lower band of discrete rising tones is seen from ~0.25 to ~0.45 f_H. The upper end of many of these rising tones appears somewhat flattened (lower df/dt) and enhanced (higher amplitude); this is common at the upper edge of the lower band of near equatorial chorus. Note the absence of activity between 0.45 and 0.55 f_H, and the low correlation of emissions between the upper and lower bands.

Chorus at 2° dipole latitude is illustrated in Fig. 7(c). The upper band of chorus and hiss now occurs

between ~0.50 and 0.65 f_H; many of the emissions appear to begin just above 0.50 f_H. (Note spurious "falling tones" at ~10 sec due to intermodulation and third harmonic distortion.) Again there is little correlation between bands.

Activity at 5° dipole latitude is shown in Fig. 7(d). Many emissions of the upper chorus band appear to begin just below or at 0.50 f_H. At this time there is an unusual degree of correlation between the bands; most of the emissions in the lower band can be associated with emissions in the upper band. However, there seems to be relatively little difference in amplitude of upper band emissions associated with weak and strong lower band emissions, suggesting that the upper band emissions may be triggered by those of the lower band rather than being simply extensions of them.

Three other representative examples of near equatorial chorus observed by OGO 3 are illustrated in Fig. 8. Double banding of chorus at the dipole equator is shown in Fig. 8(a) ($df = 5$ Hz, $K_p = 3$). The upper band extends from ~0.45 to ~0.60 f_H; the lower band from ~0.25 to ~0.40 f_H. There is little apparent correlation of individual emissions between bands. Note attenuation of the upper band by the receiver AGC when strong emissions occur in the lower band.

A case in which only a single chorus band was seen in the equatorial region is shown in Fig. 8(b) ($df = 5$ Hz, $K_p = 1$). Note that most of the strong, diffuse emissions extend from ~0.40 to ~0.65 f_H, crossing the normalized frequency of 0.45 where a gap in activity is often observed. However the gap does appear occasionally, e.g. at 21 sec.

Two emission bands observed close to the equator are shown in Fig. 8(c) ($df = 2.5$ Hz, $K_p = 2$). The upper band (~0.55 f_H) is in this case unusually narrow and appears nearly continuous but with considerable internal structure. The lower band of rising tones extending from ~0.30 to ~0.40 f_H is quite typical. Again note that the horizontal striations in these emissions do not persist longer than the 0.4 sec time resolution of the record.

Normalized frequency distributions for the 460 chorus bands observed within 9.5° of the dipole equator having simultaneous GSFC magnetometer data are shown in Fig. 9. Assuming equatorial generation in a dipole field ($f_H = 880\, L^{-3}$ kHz), we obtain the f/f_H distribution of Fig. 9(a). The distribution is broad and has a single peak near $f/f_H = 0.35$. In an earlier study (Burtis and Helliwell, 1969) based on a much smaller data sample and using the Williams and Mead (1965) model for f_H, we found that the normalized frequency of banded

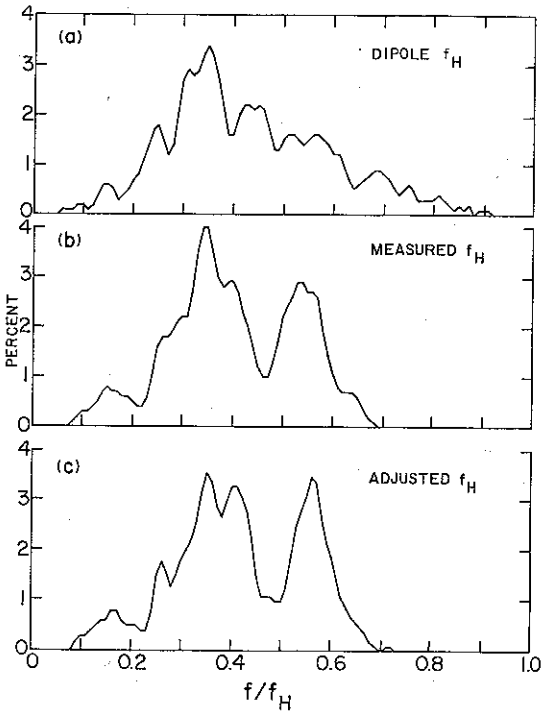

FIG. 9. NORMALIZED FREQUENCY DISTRIBUTION OF MEAN CHORUS FREQUENCY, $f = (f_{sU} f_{sL})^{1/2}$, USING THE DIPOLE MODEL FOR f_H (a), THE MEASURED VALUE OF f_H (b), AND MEASURED f_H ADJUSTED TO THE DIPOLE EQUATOR.
All data are from dipole latitudes less than 10°. Note bimodal distribution with peaks near $f/f_H = 0.35$ and 0.55.

chorus in the vicinity of the equator was usually ~0.5. Since both the dipole and Williams–Mead models can be in error by large factors in the outer magnetosphere, measured values of gyrofrequency are obviously needed.

Using the measured value of f_H provided by the onboard GSFC magnetometer, we get the distribution shown in Fig. 9(b). This distribution is considerably narrower, and two principal peaks emerge: one slightly above $f = f_H/3$ and the other slightly above $f = f_H/2$. A similar distribution was previously reported (Burtis and Helliwell, 1971) based on about 40% of the present data. Adjusting the measured f_H by a latitude factor f_{Ho}/f_H (assuming generation at 0° and dipole variation along field lines), we obtain the distribution of Fig. 9(c). The adjustment has the effect of skewing the distribution toward slightly higher normalized frequencies while narrowing the spread of the upper peak. There is no *a priori* reason to assume chorus generation exactly at 0° latitude; adjusting to some small latitude λ would simply shift the distribution of Fig. 9(c) to slightly lower normalized frequencies.

From these results we see that near equatorial

chorus tends to occur in two separate bands. Using the normalized frequency distribution of Fig. 9(c) and the median bandwidths of equatorial chorus (p. 1015), the following picture of "average" magnetospheric chorus at 0° dipole latitude emerges: a lower band of emissions at $f/f_{Ho} \cong 0.38 \pm 17\% \cong 0.31$ to 0.44; a gap at $f/f_{Ho} \cong 0.48 \pm 8\% \cong 0.44$ to 0.52; and an upper band of emissions at $f/f_{Ho} \cong 0.56 \pm 8\% \cong 0.52$ to 0.61. Individual events may show rather wide variations from the average picture. In particular, the distribution in Fig. 9(c) shows that all normalized frequencies from below 0.10 to above 0.65 were at least occasionally observed, including those typically in the range of the gap. Often only a single band of chorus (upper, lower, or indeterminate) was detected and the bandwidth varied considerably. These variations may be ascribed to many factors, including deviation of the field line minimum from the dipole equator, distortion of field lines and of f_H/f_{Ho} from the dipole model, off-equatorial generation of chorus, and variations in geomagnetic activity with associated changes in resonant electron fluxes and background concentrations. Nevertheless the bimodal normalized frequency distribution, and especially the dip just below $f/f_{Ho} = 0.5$, were persistent features of near equatorial chorus, found for all local times, L values and geomagnetic activity levels (Burtis, 1974).

Tsurutani and Smith (1974), in an OGO 5 study of postmidnight chorus below 1500 Hz, state that "in all instances of chorus examined ... no emissions at 0.50 Ω_e^- were found." In the present study, emissions crossing one-half the equatorial gyrofrequency were not uncommon (Fig. 8a,b), and the dip in the normalized frequency distribution was centreed not at $f/f_{Ho} = 0.50$, but slightly lower at $f/f_{Ho} = 0.48$. If the measured gyrofrequency is adjusted to some finite latitude rather than to the equator (e.g. 5°), then the dip occurs at an even lower frequency (e.g. $f/f_{H5} = 0.46$ assuming dipole variation along field lines). Tsurutani and Smith (1974) ascribe the extinction of half-gyrofrequency chorus to Landau damping, and Maeda (1974) suggests a sharp half-gyrofrequency absorption band due to thermal electrons. However it was found in the present study that when two chorus bands were observed, the gap between the bands did not usually seem to be caused by absorption of pre-existing emissions, since emissions in the two bands were often quite dissimilar (Figs. 7,8).

4. INTERPRETATION

For dense plasmas ($f_N \gg f_H$) there is a well known change in morphology of the whistler-mode refractive index surface at $f/f_H = 0.5$ (Helliwell, 1965). Below this critical normalized frequency the surface is convex at small wave normal angles, while above this frequency the surface is simply concave (insets, Fig. 10). At the critical frequency the curvature of the surface vanishes at zero wave normal angle. Because the ray direction is perpendicular to the refractive index surface (Budden, 1966), this suggests the possibility of enhanced phase-bunching of incoming gyroresonant electrons caused by focusing of the radiation in the direction of B_0 (Burtis and Helliwell, 1969; Helliwell and Crystal, 1973).

In the outer magnetosphere the equatorial plasma frequency f_N may at times approach the electron gyrofrequency, so it is of interest to calculate the critical frequency for these less dense plasmas. Using the full, collisionless Appleton–Hartree equation for the refractive index (Helliwell, 1965), and setting $d^2(n \cos \psi)/d\psi^2 = 0$ at wave normal angle $\psi = 0$, we obtain the condition

$$p^2 = \frac{2\Lambda_c^2(1-\Lambda_c)}{(1-2\Lambda_c)}, \qquad (1)$$

where $\Lambda_c = f/f_H$ is the critical normalized frequency and $p = f_N/f_H$ is the normalized plasma frequency. This relation, plotted in Fig. 10, indicates that the critical normalized frequency drops significantly below 0.5 when the plasma frequency falls below about twice the gyrofrequency. An approximation to this result has been reported by Bennett (1965).

To determine the radiation at a point some distance down a field line from a hypothetical source, raypaths were computed using the Stanford VLF raytracing program described and listed in a separate report (Burtis, 1975). The following model of

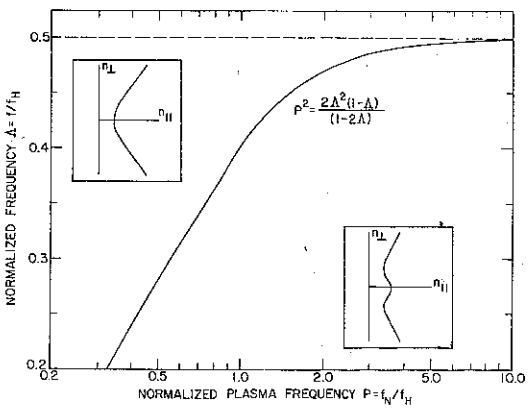

FIG. 10. CRITICAL NORMALIZED FREQUENCY AS A FUNCTION OF NORMALIZED PLASMA FREQUENCY.
Insets show morphology of the whistler-mode refractive index surface above and below the critical frequency.

the medium, in a meridional plane of the magnetosphere, was employed:

Magnetic field: dipole model, $f_{Ho} = 880\, L^{-3}$ kHz.
Electron concentration: 4.78 cm^{-3} at starting point,
r^{-4} variation (r = geocentric distance).
Starting point of rays: $L = 5.9969$,
dipole latitude = 0°.

These parameters correspond to an electron gyrofrequency of 4.08 kHz and a plasma frequency of 19.63 kHz; hence the normalized plasma frequency $f_N/f_H = 4.81$ and from Fig. 10 the critical normalized frequency $f/f_H = 0.495$. Wave frequencies were chosen to give normalized frequencies from 0.1 to 0.8, and for each normalized frequency a family of rays was computed with initial wave normal angles spaced by 5°. Two dimensional raytracing implies a line source in the east–west direction, which was isotropic in the sense that all allowable wave normals were considered to be excited.

The family of rays computed for normalized frequencies of 0.600, 0.500 and 0.400 are shown in Figs. 11(a), (b) and (c), respectively. The raypaths are shown over a range of 7° of latitude, corresponding to a distance of about 4700 km down the field line. The ordinate is L value so that straight, horizontal lines correspond to the magnetic field direction. Over this small range of latitude the spacing between field lines is relatively constant so that the ordinate may be approximated by a distance scale; this distance is exaggerated by about a factor of 10 compared to the horizontal distance, so that the range of L values shown corresponds to a distance of 260 km. By way of comparison, the whistler-mode wavelength is about 15 km, and the gyroradius of resonant electrons with 30° pitch angle is on the order of 1 km. The family of rays for a normalized frequency of 0.600, somewhat above the critical frequency, is shown in Fig. 11(a). Each ray has a different initial wave normal angle from $\psi = +45°$ to $-45°$, uniformly spaced by $\Delta\psi = 5°$. The family of rays appears similar to the corresponding case for a homogeneous medium except that all of the rays show a downward curvature. This curvature is caused almost entirely by the inhomogeneiety of the magnetic field; the small electron concentration gradient has negligible effect. Thus for a normalized frequency of 0.6, the simple concave refractive index surface gives no spatial concentration of rays, and the inhomogeneiety results in no one ray remaining parallel to B_0 over any considerable distance.

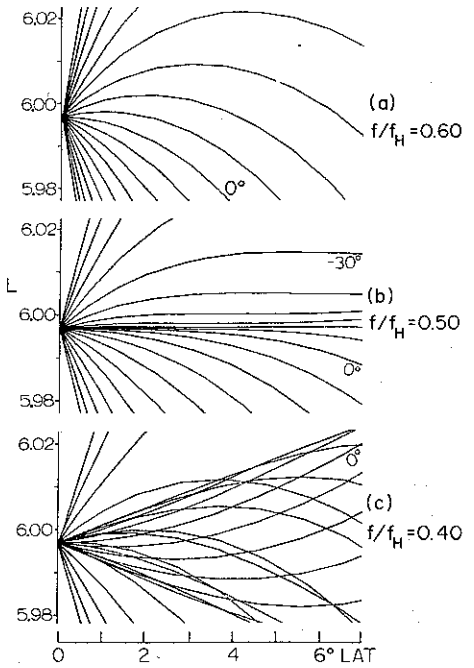

FIG. 11. COMPUTED RAYPATHS OF WAVES WITH INITIAL WAVE NORMAL ANGLES SPACED BY 5°, STARTING ON THE EQUATOR IN A MODEL MAGNETOSPHERE.

Panel a: above critical frequency, note curvature of ray paths (caused by inhomogeneity of magnetic field) and absence of focusing. Panel b: near critical frequency, rays having initial wave normal angles between 0 and −20° are focused along $L = 6$ field line. Panel c: below critical frequency, there is a caustic cone within which are two modes of radiation, the upward curving convex mode and the downward curving concave mode (see text).

In contrast Fig. 11(b) shows strong focusing and negligible curvature of some of the rays for a normalized frequency of 0.500, just above the critical value of 0.495. Again each ray has a different initial wave normal angle, uniformly spaced by $\Delta\psi = 5°$. Wave normal angles that are initially slightly inward with respect to B_0 (e.g. $\psi_0 = -10°$) rotate, because of field line curvature, outward across the flat portion of the refractive index surface, so that the ray direction (normal to the surface) remains nearly parallel to the magnetic field. This results in a concentration of rays, with initial wave normal angles between 0° and −20°, remaining parallel to or very close to the initial field line over distances of thousands of kilometers. It seems likely that in any generation mechanism involving gyroresonant interaction between counterstreaming waves and electrons, the interaction would be enhanced near this frequency and these wave normal angles.

The situation below the critical frequency (e.g.

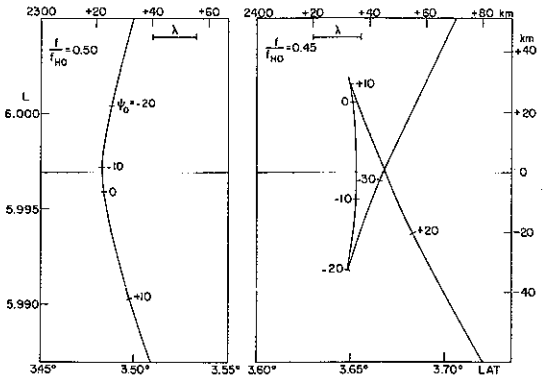

FIG. 12. COMPUTED PHASE FRONT OF WAVES AT A POINT NEARLY 2500 km DOWNFIELD FROM AN ISOTROPIC LINE SOURCE AT THE EQUATOR.

The phase front is parameterized with the initial wave normal angle of contributing rays. Note that for $f/f_{Ho} = 0.45$, below the critical frequency, the convex and concave modes are about one-half wavelength out of phase on the initial field line.

$f/f_H = 0.400$ in Fig. 11(c) is somewhat more complicated. There is a central cone of radiation about B_0 within which rays with three different wave normal angles may all propagate in the same direction (Helliwell, 1965). In particular, rays parallel to B_0 result from wave normal angles of zero and $\pm\psi_g$, where ψ_g is the Gendrin (1961) angle at which $d(n \cos \psi)/d\psi = 0$. The edge of the central cone is a type of caustic surface, and the intensity of radiation is greatest in this direction (Budden, 1966). Because of the inhomogeneous magnetic field, the ray with initial wave normal angle of 0° curves outward toward higher L values, while the rays with initial wave normal angles $\pm\psi_g$ curve inward to lower L values. Neither of these rays nor any others remains parallel to the magnetic field lines over any appreciable distance. The caustic cone is generated by wave normal angle ψ_i at the point of inflection on the refractive index surface, at which the perpendicular to the surface reaches a maximum angle with respect to B_0. In the discussion below we will refer to waves with local wave normal angle $|\psi| < \psi_i$ as the "convex mode," and $|\psi| > \psi_i$ as the "concave mode." The names are descriptive of both the refractive index surface and the phase front of the wave. Above the critical frequency only the concave mode is possible.

Phase fronts of waves at a point nearly 2500 km downfield from the source are shown in Fig. 12, as computed using the Stanford VLF raytracing programme with the inhomogeneous model described above. Along these phase fronts or "ray surfaces" all of the rays are in phase (Budden, 1966). The wave on the left, with $f/f_{Ho} = 0.50$, has a simple concave phase front, which is labelled in the figure with the initial wave normal angles of the contributing rays. The wave on the right, with $f/f_{Ho} = 0.45$, has a more complex phase front with both convex and concave modes within the caustic cone. On the initial field line, the concave mode has a slightly higher parallel component of phase velocity than the convex mode, so that at this location and normalized frequency it is about 10 km ahead of the convex mode. Also shown in the figure is the parallel component of wavelength, $\lambda_\parallel = c/(fn \cos \psi)$, and it is seen that the concave mode is close to one-half wavelength out of phase with the convex mode (the measured phase difference is 211°).

To explain the growth of narrowband waves of changing frequency we shall adopt the model of Helliwell (1967). In that model the waves phase-bunch counterstreaming cyclotron resonant electrons that in turn radiate more waves, thus creating a closed feedback loop. The stream density must exceed that for which the loop gain is unity, otherwise self-sustaining oscillations cannot occur. Frequency change is controlled primarily by the spatial rate of change of the electron gyrofrequency (see Fig. 13). A simplified computer simulation of this model shows that exponential wave growth is triggered by a short wave train applied to a resonant monoenergetic stream exceeding a threshold density (Helliwell and Crystal, 1973). Exponential

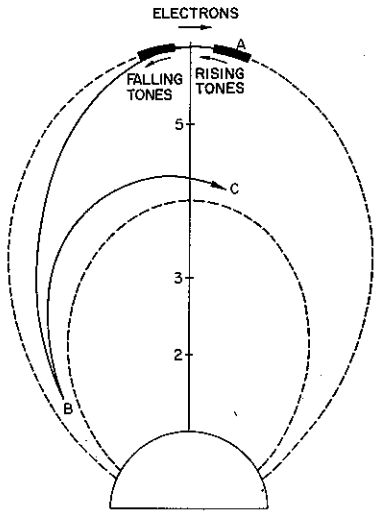

FIG. 13. SUMMARY OF MODEL IN WHICH MOST CHORUS, CONSISTING OF RISING EMISSIONS, IS GENERATED IN REGION A BY GYRORESONANT ELECTRONS.

Non-ducted emissions may be magnetospherically reflected (B) and return to equator (C); ducted emissions follow field lines to Earth.

growth in time has been observed on man-made signals transmitted from a ground VLF transmitter (Helliwell and Katsufrakis, 1974).

The model described above is one-dimensional, i.e. it assumes no variations of fields and currents in planes transverse to the static magnetic field. In a more realistic model divergence, scattering and interference would tend to restrict triggering to waves exceeding some threshold amplitude. Presumably this threshold would be a function of normalized frequency, being lowest near the critical frequency where, as shown above, waves are strongly focused along field lines and divergence loss is minimized.

Slightly below the critical frequency interference between the convex and concave modes may become important. Initially the transverse and longitudinal dimensions of the radiating region are likely to be small and the concave mode will predominate because of the larger annulus per incremental angle at larger wave normal angles. In the model of Helliwell (1967, 1970) the length of the interaction region is limited by inhomogeneity of the medium. Using the above parameters this length is found to be 2750 km, close to the distance at which the modes are 180° out of phase for $f/f_H = 0.45$. Even initially, when the size of the radiating region is small, radiated waves can interact with electrons over this entire length as determined by inhomogeneity. As the radiating region grows in length the antenna beamwidth will narrow and tend to suppress the concave mode. For example assuming the beamwidth of an endfire array, $2\phi = 2(L/2\lambda)^{-1/2}$, and a normalized frequency $f/f_H = 0.45$, the wave component at the Gendrin angle $\psi_g \cong \cos^{-1}(2f/f_H) \cong 26°$ will be at the very edge of the beamwidth for a radiator of length 165 km. When the radiating region grows to this length (about 10λ, modest compared to the interaction length of 2750 km) the convex and concave modes may be of comparable amplitude, and interference may quench further wave growth.

Well below the critical frequency the concave mode may become less important because of the large Gendrin angle. At normalized frequency $f/f_H = 0.3$, for example, $\psi_g = 53°$ and the beamwidth just includes this angle for a radiating length of 40 km. But at this normalized frequency the wavelength is 23 km, and even initially the radiator is expected to be several wavelengths long. Thus even during the initial phase of growth the concave mode may be suppressed, and emissions at these low normalized frequencies can grow in the convex mode without interference. In a smoothly varying density model the focusing at these frequencies is much less than near the critical frequency so the threshold stream density for continued wave growth is presumably higher for a given wave amplitude. Possibly the resonant electron spectrum peaks near these normalized frequencies; alternatively, field-aligned irregularities in the background concentration may limit divergence loss by guiding rays along field lines below the critical frequency. Such irregularities must be no more than several wavelengths wide to concentrate radiation strongly, and full wave theory would be required for accurate treatment of this problem (whistler ducts in the plasmasphere are thought to be wider, on the order of 400 km (Smith and Angerami, 1968)).

Burton and Holzer (1974) have measured the wave normal angle of strong chorus emissions observed on OGO 5. For about 35 dayside chorus events at normalized frequencies of 0.15–0.25 within 25° of the dipole equator (the majority of cases were within 12° of the dipole equator), they found typical wave normal angles of $-20° < \psi < -5°$. This is consistent with radiation in the convex mode. At higher latitudes there was a greater spread in the distribution of wave normal angles, although 90% of them were within 20° of the meridional plane. Many emissions had $|\psi| < 15°$ suggesting ducted propagation, while many others had $\psi > +25°$ suggesting nonducted propagation. For a single nightside pass, they interpreted the generation region as lying within 2.5° of the dipole equator. Here again most emissions in the generation region had $|\psi| < 20°$, and the behaviour of the wave normal angle farther down the propagation path clearly suggested non-ducted propagation.

The normalized frequency distribution of chorus, adjusted to the dipole equator, was found in the present study to peak at $f/f_{Ho} = 0.56$ and to dip at $f/f_{Ho} = 0.48$ (Fig. 9c). Both this upper peak and dip seem to be at a normalized frequency about 10% too high to be accounted for by our model. That is, focusing would seem to predict a peak near $\Lambda_c \cong 0.50$ and interference would seem to predict a dip near $f/f_H = 0.45$. But the distribution is based on the assumption that chorus is generated exactly at the dipole equator. If the chorus observations, which it is recalled were made over a range of ±9.5° dipole latitude, are adjusted to some finite latitude λ rather than to the equator, then the shape of the distribution will remain unchanged, but the normalized frequencies will be reduced by $f_{Ho}/f_{H\lambda}$. For the dipole model this factor reaches 10% at a latitude of 8°. In the outer magnetosphere the variation of f_H along a field line near the equator may be considerably greater than for a

dipole model because of ring current inflation (Sugiura *et al.*, 1971), so the factor may reach 10% at even lower latitudes. The above adjustment of the normalized frequency distribution assumes field-aligned propagation. While this is not strictly true for non-ducted propagation, raytracing in a dipole field shows that the change in f_{Ho} due to deviation from field lines is small compared to the change in f_H along field lines, for distances of several thousand km and small initial wave normal angles.

It was indicated above that chorus occurrence was somewhat higher at 5° latitude than at the dipole equator. Further it was shown that the occurrence of falling tones was significantly reduced within 2.5° of the dipole equator. This result supports the Helliwell (1967) model in which the latitude of the interaction region is related to the slope, df/dt, of an emission by the inhomogeneity of the medium. The majority of chorus emissions had a positive slope of ~1 kHz/sec (Fig. 5). Using the Helliwell model in a dipole field with the parameters used in the raytracing program above, and taking $df/dt = 1.0$ kHz/sec, the latitude of the interaction region is found to be 5.1°. This is reasonably close to the value inferred in the preceding paragraph, considering the uncertainties in the magnetic field configuration. It may be noted that the upper chorus band need not necessarily be centreed on the critical frequency. Since most emissions were rising in frequency, those starting near the lower edge of the band might organize electrons sufficiently to trigger emissions at higher frequencies (cf. Fig. 2c). To adjust the lower edge of the upper band from $f/f_H = 0.52$ to $f/f_H = 0.50$ requires only a 4% increase in f_H, corresponding to a dipole latitude of 5.4°.

We must now inquire whether the mechanism outlined above should apply to ducted signals observed on the ground. No evidence of an attenuation band just below $f_{Ho}/2$ has been reported for ground-based data. It is observed that ducted emissions are often triggered by other signals (whistlers, power line radiation, VLF transmitters, echoes of previous emissions). Assuming that the wave front of the triggering signal has a lateral dimension of many wavelengths (a typical duct is 400 km across at the equator and a typical wavelength is 5 km), we would not expect to excite any significant components of the concave mode. Thus there would be no interference and hence no gap.

An interesting test of the above interpretation of the bimodal normalized frequency distribution of magnetospheric chorus would involve studying the chorus frequency at times when the normalized plasma frequency, f_N/f_H, is depressed. For example, if $f_N/f_H = 1$ the morphological change in the whistler mode refractive index surface occurs at $f/f_H = 0.4$, and the normalized frequency of the upper chorus band should correspondingly be depressed by 20%. Interpretations not involving the morphological change of the refractive index surface would not predict this change in frequency. Conditions of low f_N/f_H might be expected quite often just outside the plasmapause following magnetic storms. Unfortunately the OGO 3 orbit did not cover the equatorial region at low L values (Fig. 1), so this test could not be conducted with the present data.

In summary, most magnetospheric chorus consists of rising emissions, which are probably generated by gyroresonant electrons slightly off the equator (region A in Fig. 13). These emissions are often generated in two bands: an upper band at the critical frequency f/f_H ~0.5 where focusing is maximized, and a lower band at a frequency that may perhaps correspond to a peak in the flux of gyroresonant electrons. Modal interference may contribute to the gap between the two bands. Occasional falling tones are generated on the opposite side of the equator, and, as seen in Fig. 13, travel poleward without crossing the equator. Non-ducted emissions are refracted inward to slightly lower L shells as they propagate Earthward (Burtis and Helliwell, 1969), and may be magnetospherically reflected (region B in Fig. 13). In principle they can return to the equator at lower L (region C, f/f_H ~0.2) and perhaps trigger new emissions. However the returning wave may be highly attenuated by Landau damping and to date has not been observed. Other emissions may become ducted and propagate along field lines (dashed curves in Fig. 13) to the lower ionosphere.

Acknowledgements—Discussions with our colleagues, especially Drs. T. F. Bell and D. L. Carpenter, were invaluable aids at various points in this research. We are grateful to Dr. J. P. Heppner for the use of the Goddard Space Flight Center Rb vapor magnetometer data.

This work was supported by the National Aeronautics and Space Administration under Grant NGL-05-020-008.

REFERENCES

Allcock, G. McK. (1957). A study of the audio-frequency radio phenomenon known as "dawn chorus". *Aust. J. Phys.* **10,** 286.

Allcock, G. McK. and Mountjoy, J. C. (1970). Dynamic spectral characteristics of chorus at a middle-latitude station. *J. geophys. Res.* **75,** 2503.

Bennett, S. M. (1965). An improved whistler-mode refractive index equation. *J. geophys. Res.* **70,** 725.
Brice, N. M. (1964). Fundamentals of very low frequency emission generation mechanisms. *J. geophys. Res.* **69,** 4515.
Brinca, A. L. (1972a). On the stability of obliquely propagating whistlers. *J. geophys. Res.* **77,** 3495.
Brinca, A. L. (1972b). Whistler side-band growth due to nonlinear wave-particle interaction. *J. geophys. Res.* **77,** 3508.
Budden, K. G. (1966). *Radio Waves in the Ionosphere.* Cambridge University Press, London.
Burrows, J. R. and McDiarmid, I. B. (1972). Trapped particle boundary regions. In *Critical Problems of Magnetospheric Physics* (Ed. E. R. Dyer), pp. 83–106. IUCSTP Secretariat, National Acad. Sci., Washington, DC.
Burtis, W. J. (1969). Magnetic radiation observed by the OGO-1 and OGO-3 broadband vlf receivers, Rept. No. SEL 69-019, Radioscience Lab., Stanford Electronics Labs., Stanford University, Stanford, CA.
Burtis, W. J. (1973). Electron concentrations calculated from the lower hybrid resonance noise band observed by OGO 3. *J. geophys. Res.* **78,** 5515.
Burtis, W. J. (1974). Magnetospheric chorus, Rept. No. SEL 74-041. Radioscience Lab., Stanford Electronics Labs., Stanford University, Stanford, CA.
Burtis, W. J. (1975). Users' guide to the Stanford vlf raytracing program. Internal Rept. Radioscience Lab., Stanford University, Stanford, CA.
Burtis, W. J. and Helliwell, R. A. (1969). Banded chorus—a new type of vlf radiation observed in the magnetosphere by OGO 1 and OGO 3. *J. geophys. Res.* **74,** 3002.
Burtis, W. J. and Helliwell, R. A. (1971). Normalized frequency of vlf banded chorus near the equator. *Trans. AGU.* **52,** 332.
Burtis, W. J. and Helliwell, R. A. (1975). Magnetospheric chorus: amplitude and growth rate. *J. geophys. Res.* **80,** 3265.
Burton, R. K. and Holzer, R. E. (1974). The origin and propagation of chorus in the outer magnetosphere. *J. geophys. Res.* **79,** 1014.
Carpenter, D. L. (1967). Relations between the dawn minimum in the equatorial radius of the plasmapause and D_{st}, K_p, and local K at Byrd Station. *J. geophys. Res.* **72,** 2969.
Coroniti, F. V., Fredricks, R. W. Kennel, C. F. and Scarf, F. L. (1971). Fast time resolved spectral analysis of vlf banded emissions. *J. geophys. Res.* **76,** 2366.
Crouchley, J. and Brice, N. M. (1960). A study of "chorus" observed at Australian stations. *Planet. Space Sci.* **2,** 238.
Dunckel, N. and Helliwell, R. A. (1969). Whistler-mode emissions on the OGO 1 satellite. *J. geophys. Res.* **74,** 6371.
Dysthe, K. B. (1971). Some studies of triggered whistler emissions. *J. geophys. Res.* **76,** 6915.
Ficklin, B. P., Stehle, R. H., Barnes, C. and Mills, M. E. (1967). The instrumentation for the Stanford University/Stanford Research Institute vlf experiment (B-17) on the OGO-3 satellite, supplemental report. Stanford Res. Inst., Menlo Park, CA.
Frandsen, A. M. A., Holzer, R. E. and Smith, E. J. (1969). OGO search coil magnetometer experiments. *IEEE Trans. Geosci. Electronics,* **GE-7,** 61.
Gallet, R. M. (1959). The very low frequency emissions generated in the earth's exosphere. *Proc. IRE,* **47,** 211.
Gendrin, R. (1961). Le guidage des whistlers par le champ magnetique. *Planet. Space Sci.* **5,** 274.
Gurnett, D. A. and O'Brien, B. J. (1964). High-latitude geophysical studies with the satellite Injun-3; 5. Very-low-frequency electromagnetic radiation. *J. geophys. Res.* **69,** 65.
Hartz, T. R. and Brice, N. M. (1967). The general pattern of auroral particle precipitation. *Planet. Space Sci.* **15,** 301.
Helliwell, R. A. (1960). Summary of research on whistlers and related phenomena. *J. Res. NBS,* **64D,** 642.
Helliwell, R. A. (1965). *Whistlers and Related Ionospheric Phenomena,* Stanford University Press, Stanford, CA.
Helliwell, R. A. (1967). A theory of discrete vlf emissions from the magnetosphere. *J. geophys. Res.* **72,** 4773.
Helliwell, R. A. (1970). Intensity of discrete vlf emissions, *Particles and Fields in the Magnetosphere* (Ed. B. M. McCormac), pp. 292–301, Reidel, Dordrecht, Holland.
Helliwell, R. A. and Crystal, T. L. (1973). A feedback model of cyclotron interaction between whistler-mode waves and energetic electrons in the magnetosphere. *J. geophys. Res.* **78,** 7357.
Helliwell, R. A., Katsufrakis, J., Trimpi, M. and Brice, N. (1964). Artificially stimulated very-low-frequency radiation from the ionosphere. *J. geophys. Res.* **69,** 2391.
Kennel, C. F. and Petscheck, H. E. (1966). Limit on stably trapped particle fluxes. *J. geophys. Res.* **71,** 1.
Laaspere, T., Morgan, M. G. and Johnson, W. C. (1964). Chorus, hiss and other audiofrequency emissions at stations of the whistlers-east network. *Proc. IEEE,* **52,** 1331.
Maeda, K. (1974). Electron cyclotron side band emissions. *Trans. AGU,* **55,** 398.
Muzzio, J. L. R. and Angerami, J. J. (1972). OGO 4 observations of extremely low frequency hiss. *J. geophys. Res.* **77,** 1157.
Nunn, D. (1971). A theory of vlf emissions, *Planet. Space Sci.* **19,** 1141.
Nunn, D. (1974). A theoretical investigation of banded chorus. *J. Plasma Phys.* **11,** 189.
Pope, J. H. (1963). A high-latitude investigation of the natural very-low-frequency electromagnetic radiation known as chorus. *J. geophys. Res.* **68,** 83.
Russell, C. T., Holzer, R. E. and Smith, E. J. (1969). OGO 3 observations of elf noise in the magnetosphere; 1, spatial extent and frequency of occurrence. *J. geophys. Res.* **74,** 755.
Smith, R. L. and Angerami, J. J. (1968). Magnetospheric properties deduced from OGO 1 observations of ducted and nonducted whistlers. *J. geophys. Res.,* **73,** 1.
Stiles, G. S. (1975). Comment on a paper by Coroniti, Fredricks, Kennel and Scarf, "Fast time resolved spectral analysis of vlf banded emissions:" *J. geophys. Res.* **80,** 4401.
Stiles, G. S. and Helliwell, R. A. (1975). Initial frequency-time behaviour of artificially stimulated vlf emissions. *J. geophys. Res.* **80,** 608.
Storey, L. R. O. (1953). An investigation of whistling atmospherics. *Phil. Trans. R. Soc. (London) (A)* **246,** 133.
Sudan, R. N. and Ott, E. (1971). Theory of triggered vlf emissions. *J. geophys. Res.* **76,** 4463.
Sugiura, M., Ledley, B. G., Skillman, T. L. and Heppner,

J. P. (1971). Magnetospheric-field distortions observed by OGO 3 and 5. *J. geophys. Res.* **76,** 7552.
Taylor, W. W. L. and Gurnett, D. A. (1968). Morphology of vlf emissions observed with the Injun 3 satellite. *J. geophys. Res.* **73,** 5615.
Tsurutani, B. T. and Smith, E. J. (1974). Postmidnight chorus: a substorm phenomenon, *J. geophys. Res.* **79,** 118.
Williams, D. J. and Mead, G. D. (1965). Nightside magnetosphere configuration as obtained from trapped electrons at 1100 kilometers. *J. geophys. Res.* **70,** 3017.